

Pilot Study Assessing the Impact of Intrathecal Administration of Variants AAV-PHP.B and AAV-PHP.eB on Brain Transduction in Adult Rhesus Macaques

Marie-Laure Arotcarena, Sandra Dovero, Nathalie Biendon, Nathalie Dutheil, Vincent Planche, Erwan Bezard, Benjamin Dehay

▶ **To cite this version:**

Marie-Laure Arotcarena, Sandra Dovero, Nathalie Biendon, Nathalie Dutheil, Vincent Planche, et al.. Pilot Study Assessing the Impact of Intrathecal Administration of Variants AAV-PHP.B and AAV-PHP.eB on Brain Transduction in Adult Rhesus Macaques. Frontiers in Bioengineering and Biotechnology, 2021, 9, 10.3389/fbioe.2021.762209 . inserm-03429973

HAL Id: inserm-03429973

https://inserm.hal.science/inserm-03429973

Submitted on 16 Nov 2021

HAL is a multi-disciplinary open access archive for the deposit and dissemination of scientific research documents, whether they are published or not. The documents may come from teaching and research institutions in France or abroad, or from public or private research centers.

L'archive ouverte pluridisciplinaire **HAL**, est destinée au dépôt et à la diffusion de documents scientifiques de niveau recherche, publiés ou non, émanant des établissements d'enseignement et de recherche français ou étrangers, des laboratoires publics ou privés.

frontiers in Bioengineering and Biotechnology

ORIGINAL RESEARCH
published: 15 November 2021
doi: 10.3389/fbioe.2021.762209

Pilot Study Assessing the Impact of Intrathecal Administration of Variants AAV-PHP.B and AAV-PHP.eB on Brain Transduction in Adult Rhesus Macaques

*Marie-Laure Arotcarena[1], Sandra Dovero[1], Nathalie Biendon[1], Nathalie Dutheil[1], Vincent Planche[1,2], Erwan Bezard[1] and Benjamin Dehay[1]**

[1]CNRS, IMN, UMR 5293, Univ. Bordeaux, Bordeaux, France, [2]Centre Memoire de Ressources et de Recherches, Pôle de Neurosciences Cliniques, CHU de Bordeaux, Bordeaux, France

Adeno-associated virus (AAV) vectors are increasingly used as an effective and safe approach to deliver genetic material to the central nervous system (CNS). The AAV9-derived variants, AAV-PHP. B and AAV-PHP.eB, reportedly broadly transduce cells throughout the CNS compared to the original serotype 9, AAV9. As non-human primate data are scarce, we here evaluated the CNS transduction efficiencies after lumbar intrathecal bolus delivery of identical doses of either AAV-PHP. B:CAG-EGFP or AAV-PHP. eB:CAG-EGFP in rhesus macaque monkeys. AAV-PHP.eB achieved a more efficient and widespread CNS transduction compared to AAV-PHP.B. We report a strong neuronal and oligodendroglial tropism for both variants in the putamen and in the hippocampus. This proof-of-concept experiment highlights the potential value of intrathecal infusions of AAV-PHP.eB to distribute genetic material in the CNS with cell-type specificity and introduces a new opportunity to model brain diseases in rhesus macaque monkeys and further develop gene therapies targeting the CNS in humans.

Keywords: adeno-associated virus, intrathecal injection, CNS, non-human primate, animal model

OPEN ACCESS

Edited by:
Liliana Simões Mendonça, University of Coimbra, Portugal

Reviewed by:
Nihay Laham Karam, University of Eastern Finland, Finland
Sandro Alves, Brainvectis Therapeutics, France

****Correspondence:***
Benjamin Dehay
benjamin.dehay@u-bordeaux.fr

Specialty section:
This article was submitted to Preclinical Cell and Gene Therapy, a section of the journal Frontiers in Bioengineering and Biotechnology

Received: *21 August 2021*
Accepted: *26 October 2021*
Published: *15 November 2021*

Citation:
Arotcarena M-L, Dovero S, Biendon N, Dutheil N, Planche V, Bezard E and Dehay B (2021) Pilot Study Assessing the Impact of Intrathecal Administration of Variants AAV-PHP.B and AAV-PHP.eB on Brain Transduction in Adult Rhesus Macaques. Front. Bioeng. Biotechnol. 9:762209. doi: 10.3389/fbioe.2021.762209

INTRODUCTION

The use of non-pathogenic adeno-associated virus (AAV) vectors has emerged as an effective and safe approach for both preclinical modeling and therapeutic methods for neurological disorders (Bourdenx et al., 2014; Deverman et al., 2018; Hudry and Vandenberghe, 2019; Nectow and Nestler, 2020; Fajardo-Serrano et al., 2021). In particular, specific serotypes of AAV, such as recombinant adeno-associated virus serotype 9 (AAV9) and pseudotype rhesus-10 (AAVrh.10), have shown unique properties to target the central nervous system (CNS) in comparison to most AAV serotypes (Foust et al., 2009). Since both serotypes share the ability to cross the blood-brain barrier (BBB) in newborns, they may be delivered through various administration routes (Bourdenx et al., 2014; Bedbrook et al., 2018). They are associated with widespread, long-term transduction in nondividing cells in rodents (Cearley and Wolfe, 2006; Duque et al., 2009; Foust et al., 2009; Zhang et al., 2011; Chansel-Debordeaux et al., 2017; Chansel-Debordeaux et al., 2018) and non-human primates (NHPs) (Dehay et al., 2012; Gray et al., 2013; Samaranch et al., 2013; Hinderer et al., 2014; Yang et al., 2014; Bey et al., 2020), making them a powerful tool for delivering genetic material to the

CNS. Recently, a novel AAV9-derived variant that far more efficiently crosses the mouse BBB (named AAV-PHP. B) has been identified by screening a library of AAV9 vectors carrying random mutations at the capsid surface (Deverman et al., 2016). AAV-PHP. B transfers genetic information throughout the CNS with high efficiency compared to the gold-standard AAV9 (Deverman et al., 2016) and transduces most brain cells (approximately 50–100% of neurons and 80% of astrocytes) across multiple CNS regions after peripheral delivery in mice (Deverman et al., 2016; Allen et al., 2017; Gao et al., 2017; Morabito et al., 2017; Hordeaux et al., 2018; Rincon et al., 2018) and rats (Jackson et al., 2016). However, at odds with rodent data, intravenously delivered AAV-PHP. B did not demonstrate the same capabilities in both marmosets (6 weeks survival) (Matsuzaki et al., 2018) and rhesus macaques (3 weeks survival) (Hordeaux et al., 2018).

Pursuing the effort towards identification of AAVs with tremendous transduction potential, the group that discovered AAV-PHP. B recently reported an enhanced AAV-PHP. B variant (AAV-PHP.eB) that shows further improvements in neurons and glia transduction efficiency throughout the CNS after intravenous delivery in adult mice (Chan et al., 2017; Mathiesen et al., 2020), or after intravascular (Dayton et al., 2018) and cisterna magna (Chatterjee et al., 2021) administration in adult rats. As a face-to-face comparison of AAV-PHP. B and AAV-PHP. eB is currently missing in NHP, we here compared the CNS transduction efficacy of these two new variants after intrathecal injection of the same dose in the rhesus macaque (*Macaca mulatta*). Using the EGFP reporter transgene to characterize viral biodistribution, we observe enhanced AAV-PHP. eB-mediated viral transduction compared to AAV-PHP. B throughout the CNS. Furthermore, we report a neuronal and oligodendroglial tropism for both variants in the NHPs brain.

MATERIALS AND METHODS

Animals

Two female adult rhesus monkeys (*Macaca mulatta*), weighing ~6–7 kg (9–10 years old), were used in this study. The monkeys were housed in the animal facility of the Institute of Neurodegenerative Diseases (UMR CNRS 5293) under standard conditions (12/12 h day/night cycle, ~60% humidity, and ~22°C). All experimental protocols comply with the Council Directive of 2010 (2010/63/EU) of the European Community and the National Institute of Health Guide for the Care and Use of Laboratory Animals. The proposed research has received French Ethical Committee for Animal Research CE50 (agreement number: 12286).

Viral Vectors and Surgical Procedures

Production of the Viral Vector

Recombinant AAV vectors (rAAV) were produced at the vector core facility of our lab. rAAV were generated by polyethylenimine mediated triple transfection of low passage HEK-293T/17 cells (ATCC; cat number CRL-11268). The AAV expression plasmid pAAV2-CAG-EGFP-WPRE-pA (enhanced green fluorescent protein (EGFP) under the control of cytomegalovirus enhancer fused to the chicken beta-actin (CAG) promoter) was co-transfected with plasmids encoding the AAV2 rep and AAV-PHP. B or AAV-PHP. eB cap genes (pUCmini-iCAP-PHP.B, Addgene # 103,002; pUCmini-iCAP-PHP.eB, Addgene # 103005) and adenoviral helper functions (pAdΔF6, Addgene # 112867) (Xiao et al., 1998). AAV vectors were purified as previously described (Zolotukhin et al., 2002). Cells were harvested 72 h post-transfection, resuspended in lysis buffer (150 mM NaCl, 50 mM Tris-HCl pH 8.5), and lysed by three freeze-thaw cycles (37°C/−80°C). The cell lysate was treated with 150 units/ ml Benzonase (Sigma Aldrich, St Louis, MO, United States) for 1 h at 37°C, and the crude lysate was clarified by centrifugation. Vectors were purified by iodixanol step gradient centrifugation and concentrated and buffer-exchanged into Lactated Ringer's solution (Baxter, Deerfield, IL, United States) using vivaspin20 100 kDa cut off concentrator (Sartorius Stedim, Goettingen, Germany). Titrations were performed at the platform study of the transcriptome (Neurocentre Magendie, INSERM U862, Bordeaux, France). The genome-containing particle (gcp) titer was determined by quantitative real-time PCR using the Light Cycler 480 SYBR green master mix (Roche, cat # 04887352001) with primers specific for the AAV2 ITRs (fwd 5′-GGAACCCCTAGTGATGGAGTT-3′; rev 5′-CGGCCTCAG TGAGCGA-3′) (Aurnhammer et al., 2012) on a Light Cycler 480 instrument. Purity assessment of vector stocks was estimated by loading 10 µL of vector stock on 10% SDS acrylamide gels. According to the manufacturer's instructions, total proteins were visualized using the Krypton Infrared Protein Stain (Life Technologies). The production and the titration for both AAV9-derived variants have been made in parallel to avoid any bias.

Intrathecal Injections

Injections were performed under aseptic conditions and isoflurane and O_2 deep anaesthesia, following induction with ketamine (10 mg/ IM) and atropine (0.05 mg/ kg IM). Body temperature, heart rate, blood pressure, and SpO_2 were monitored throughout all procedures. The injection site has been prepared by initially wiping the area with sponges soaked in 70% isopropyl alcohol and/ or betadine scrub, allowed to dry. The animal was placed in lateral recumbence, and a 22G cannula for lumbar puncture was introduced into the L4-L5 intrathecal space. The presence of CSF in the cannula after the removal of the stylet certified the intrathecal placement. A solution containing AAV-PHP. B:CAG-EGFP-WPRE-pA was then injected at 1.0×10^{12} vg for one monkey, corresponding to 180 µL. A solution containing AAV-PHP. eB:CAG-EGFP-WPRE-pA was injected at 1.0×10^{12} vg per monkey, corresponding to 100 µL. The intrathecal administration was followed by a flush of 0.4 ml of sterile saline. The cannula was removed, and the animal was maintained in lateral recumbence for 1 hour until recovery from anaesthesia. Animals were longitudinally followed and euthanized 2 months post-injection.

Post-Mortem Processing

Animals were deeply anesthetized with a lethal dose of pentobarbital (50 mg/kg) and transcardially perfused with room-temperature 0.9% saline solution (containing 1%

TABLE 1 | Summary of study subjects.

Animal #	Virus	Sex	Age (year)	Weight at injection (kg)	Viral titers (vg/ml)	Volume (µL)	Dose (vg/kg)	Sacrifice (days after injection)
1	PHP.B	female	9.6	6,5	5.33×10^{12}	180	1.5×10^{11}	60
2	PHP.eB	female	9.7	6,7	1.04×10^{13}	100	1.5×10^{11}	60

heparin) following accepted European Veterinary Medical Association guidelines. Brains, spinal cords, and livers were removed quickly after death. Each brain was then dissected along the midline, and each hemisphere was divided into three parts. Each spinal cord was divided into three parts (cervical thoracic, lumbar). These tissues were postfixed in a large volume of 4% buffered paraformaldehyde solution for 1 week at 4°C and cryoprotected in successive baths of 20–30% sucrose solution diluted in 0.1 M phosphate buffered saline (PBS) at 4°C until they sunk. Finally, brains were frozen by immersion in an isopentane bath at −55°C for 5 min and stored immediately at −80°C until sectioning. No samples were excluded from analysis in these studies.

Immunohistochemical Analysis

Transgene Expression

Brains, spinal cords and livers were sectioned in 50 µm thick serial free-floating coronal sections in a Leica CM3050S cryostat (Leica Microsystems, Wetzlar, Germany) at −20°C, collected in PBS Azide 0.2% and store at 4°C until they were processed for EGFP immunoreactivity. Coronal free-floating sections were incubated with a mouse monoclonal antibody raised against GFP (Invitrogen Anti-GFP Monoclonal (3E6), Catalog #A-11120; 1:1000) for one night at room temperature and revealed by an anti-mouse peroxidase EnVision™ system (DAKO, K4011) followed by DAB incubation. Free-floating sections were then mounted on gelatinized slides, counterstained with cresyl violet, dehydrated, and coverslipped before further analysis. Sections were scanned in a high-resolution scanner (PanScan, 3D Histech) at ×20 magnification, and the quantification of GFP-positive signal was estimated by an immunostaining-positive surface quantification in the different brain regions with the Mercator software (Explora Nova). All analyses were performed blinded to the researcher.

Immunofluorescence Analysis

To assess brain cellular subtype markers (i.e., neurons, microglia, astrocytes, and oligodendrocytes) co-expressed with EGFP, striatal and hippocampal monkey sections were incubated simultaneously with two antibodies: a chicken polyclonal antibody against GFP (Abcam, ab13970, 1:1000) and, respectively, a mouse monoclonal antibody against NeuN (Millipore, Darmstadt, Germany, MAB377, 1:1000) or a rabbit monoclonal against human Iba1 (FUJIFILM Wako Pure Chemical Corporation, 019-19741, 1:1000) or a mix of mouse monoclonal antibodies against GFAP and S-100 (Sigma-Aldrich (clone GA5), 1:2000/Abcam, ab7852, 1:1000) or a mouse monoclonal antibody against CNPase (Abcam, ab237961, 1: 1000) for one night at room temperature. Incubation with secondary antibodies was done sequentially with a goat anti-chicken AlexaFuor 488 (Abcam, A11039, 1:400) and a goat anti-mouse AlexaFluor 568 (Invitrogen, A11031, 1:400) or a goat anti-rabbit AlexaFluor 568 (Invitrogen, A11036, 1:400) 1h30 at room temperature. Sections were mounted on non-gelatinized slides and coverslipped using fluorescent mounting media without DAPI (Vector Labs). Images were acquired using a Zeiss SP5 confocal microscope.

Quantitative Analysis

For each NHP, one slice of the median part of the striatal or the hippocampal level was selected for each cell-type-specific marker/EGFP double-labeling immunofluorescence. Ten to thirteen images were captured at ×40 magnification with a confocal laser microscope (LSM780; Zeiss). Cellular tropism is reported as a percentage of total EGFP-positive or EGFP-negative cells per cell type counted in all images acquired [corresponding to a total of NeuN-positive (92–119 cells in the striatum, 116–124 cells in the hippocampus), Iba1-positive (33–45 cells in the striatum, 36–43 cells in the hippocampus), GFAP/S-100-positive (33–47 cells in the striatum, 84–83 cells in the hippocampus), CNPase-positive (101–111 cells in the striatum, 32–71 cells in the hippocampus) cells]. The percentage corresponds to the proportion of EGFP-positive or EGFP-negative cell divided by the total number of counted cells, calculated independently for each cell type. For example, for the percentage of transduced neurons, we calculated the number of EGFP-positive neurons divided by the total number of analysed neurons expressed in percentage.

Biochemical Analysis

Protein Extraction

We used 2 mm^3 formalin-fixed tissue per animal. Tissue patches were extracted using the Qproteome FFPE Tissue Kit (Qiagen), and then quantified using the Lowry method (Biorad RC DC Protein Assay Kit) following the manufacturer's instructions. Based on total protein concentrations calculated from the assay, aliquots of tissue lysates corresponding to 10 µg were prepared for each structure in Laemmli buffer (Tris-HCl 25 mM pH = 6.8, glycerol 7.5%, SDS 1%, DTT 250 mM and bromophenol blue 0.05%). Samples were loaded into 12% SDS-PAGE gel, followed by electrophoretic transfer onto 0.2 l m nitrocellulose membranes (Bio-Rad, Hercules, CA, United States). Membranes were blocked in phosphate buffer saline (PBS) with 5% dry skimmed milk and probed with antibodies against GFP (JL-8; Clontech, Mountain View, CA, Living Colors, 1:1000) overnight. Anti-actin (1:5,000; Sigma) was used to control equal loading. Appropriate secondary antibodies coupled to peroxidase were revealed using a Super Signal West Pico Chemiluminescent kit (Immobilon Western, Chemiluminescent HRP substrate, Millipore) and analysed with Image Lab software 5.0 (Bio-Rad, Hercules, United States).

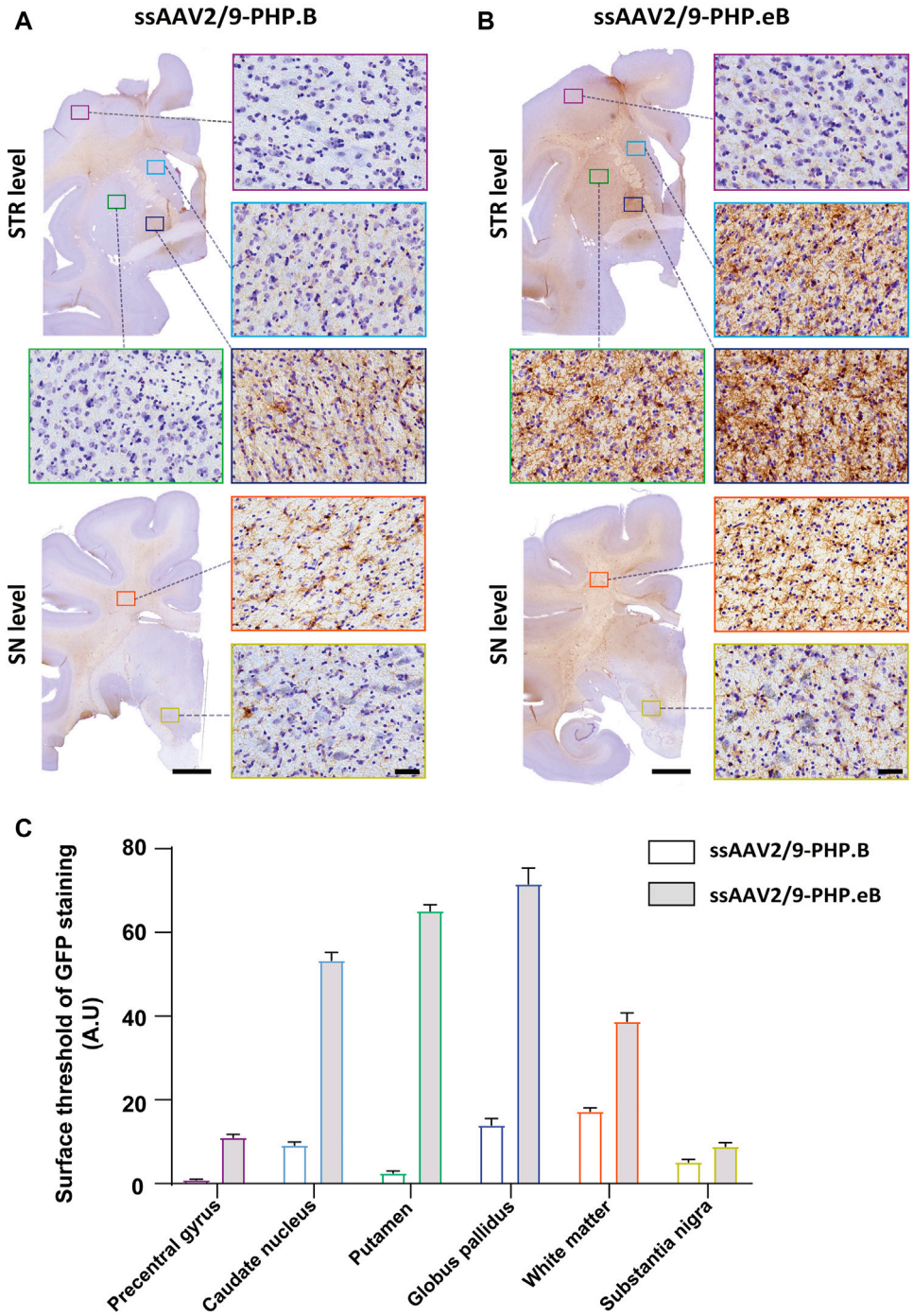


FIGURE 1 | Stronger widespread brain EGFP distribution after intrathecal injection of AAV-PHP. eB compared to variants AAV-PHP. B in non-human primates. **(A–B)** Representative coronal brain sections at two different rostrocaudal levels (top, "STR" = striatal level, AC0; bottom, "SN" = Substantia Nigra level, AC-8) of EGFP immunostaining (left) and illustrative photomicrographs (right) of EGFP immunostaining in the precentral gyrus (purple square), in the caudate nucleus (light blue square), in the putamen (green square), in the globus pallidus (dark blue square), in the white matter (orange square) and the substantia nigra (yellow square) in monkeys injected with either AAV-PHP. B **(A)** or AAV-PHP. eB **(B)**. Scale bars = 5 mm (left, sections) and 40 μm (right, insets). **(C)** Quantitative analysis of GFP immunostaining measured by the surface threshold in all analyzed regions, including the precentral gyrus, the caudate nucleus, the putamen, the globus pallidus, the white matter, and the substantia nigra in AAV-injected monkeys. Data represent mean ± SEM.

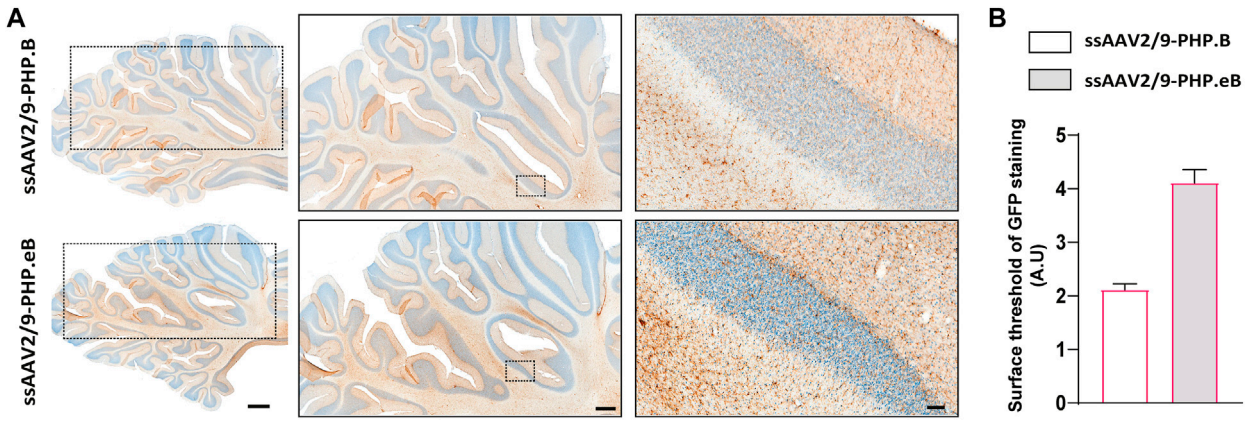


FIGURE 2 | Stronger widespread brain EGFP distribution after intrathecal injection of AAV-PHP. eB compared to variants AAV-PHP. B in the cerebellum of non-human primates. **(A)** Representative coronal brain sections at the cerebellum level (AC-17 mm) of EGFP immunostaining (left) and illustrative photomicrographs (middle and right) of EGFP immunostaining in the cerebellum in monkeys injected with either AAV-PHP. B (up) or AAV-PHP. eB (down). Scale bars = 2 mm (left, sections), 1 mm (middle, sections) and 100 µm (right, insets). **(B)** Quantitative analysis of EGFP immunostaining measured by surface threshold analyzed on four sections of the cerebellum in AAV-injected monkeys. Data represent mean ± SEM.

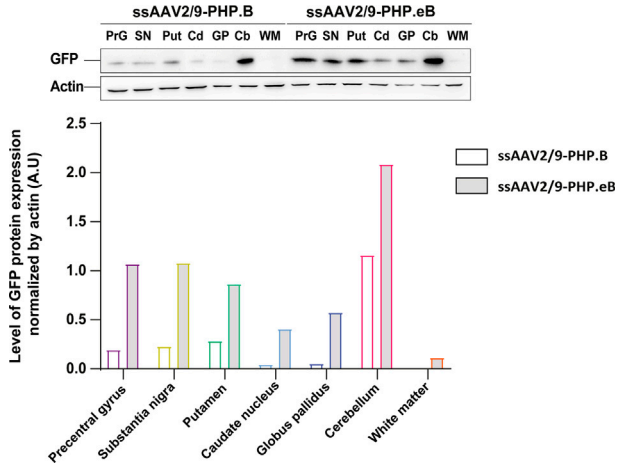


FIGURE 3 | Stronger widespread brain EGFP distribution after intrathecal injection of AAV-PHP. eB compared to variants AAV-PHP.B. Representative images and quantification of EGFP expression analyzed across brain lysates of AAV-injected monkeys.

RESULTS

AAV-PHP.eB:CAG-EGFP Displayed Greater GFP Transduction Efficiency

To confirm the ability of AAV9-derived variants, AAV-PHP. B and AAV-PHP. eB, to transduce neural cells after intrathecal delivery, we proceeded with a pilot study in NHPs (**Table 1**). Naïve 9-to 10-year-old adult rhesus macaques (n = 1 per vector) received single intrathecal injections of viruses at a dose of 1.0×10^{12} vector genomes (vg) per animal (1.5×10^{11} vg/ kg body weight), a quantity that was comparable with the highest dose used in the mouse studies (Chan et al., 2017). Both NHPs tolerated the vectors well. Two months later, both monkeys were euthanized. We first qualitatively evaluated the relative transduction profiles of AAV-PHP. B:CAG-EGFP (**Figure 1A**) and AAV-PHP. eB: CAG-EGFP (**Figure 1B**). The monkey injected with AAV-PHP. eB:CAG-EGFP showed an extensive CNS transduction and a more intense expression of EGFP throughout the brain than the monkey injected with AAV-PHP. B:CAG-EGFP. A quantitative unbiased evaluation of the EGFP-positive cell surface staining confirmed these observations (**Figure 1C**). Several cortical and subcortical structures such as the precentral gyrus, the putamen, the caudate nucleus, the globus pallidus, the white matter, and the substantia nigra showed EGFP staining suggesting transduction of these structures by both variants. Deeper brain structures (such as the putamen, the caudate nucleus and the globus pallidus) were even more EGFP-positive in AAV-PHP. eB-injected monkey. Similarly, a broad viral transduction was observed in the cerebellum for both variants with stronger EGFP-positive staining observed for the AAV-PHP. eB-injected monkeys (**Figures 2A,B**). Immunoblots of the same brain areas showed significantly higher levels of EGFP expression in the AAV. PHP.eB-injected monkey compared to that of AAV.PHP.B-injected monkey (**Figure 3**).

Both Vectors Achieved a Neuronal and Oligodendroglial Tropism in the Putamen

Since the CAG promoter is ubiquitous, we attempted to evaluate whether the transgene expression was detected in different cell types (i.e., neuronal and glial cells). Immunofluorescence double-staining analyses were performed at the striatum level, where the transduction efficiency was one of the strongest. In the putamen, in both AAV-PHP. B (**Figure 4A**) and AAV-PHP. eB (**Figure 4B**) conditions, double immunolabeling with the pan-neuronal marker NeuN or the well-established oligodendrocyte marker CNPase showed that EGFP was expressed predominantly in neurons and oligodendrocytes, suggesting a neuronal tropism. Scarce co-

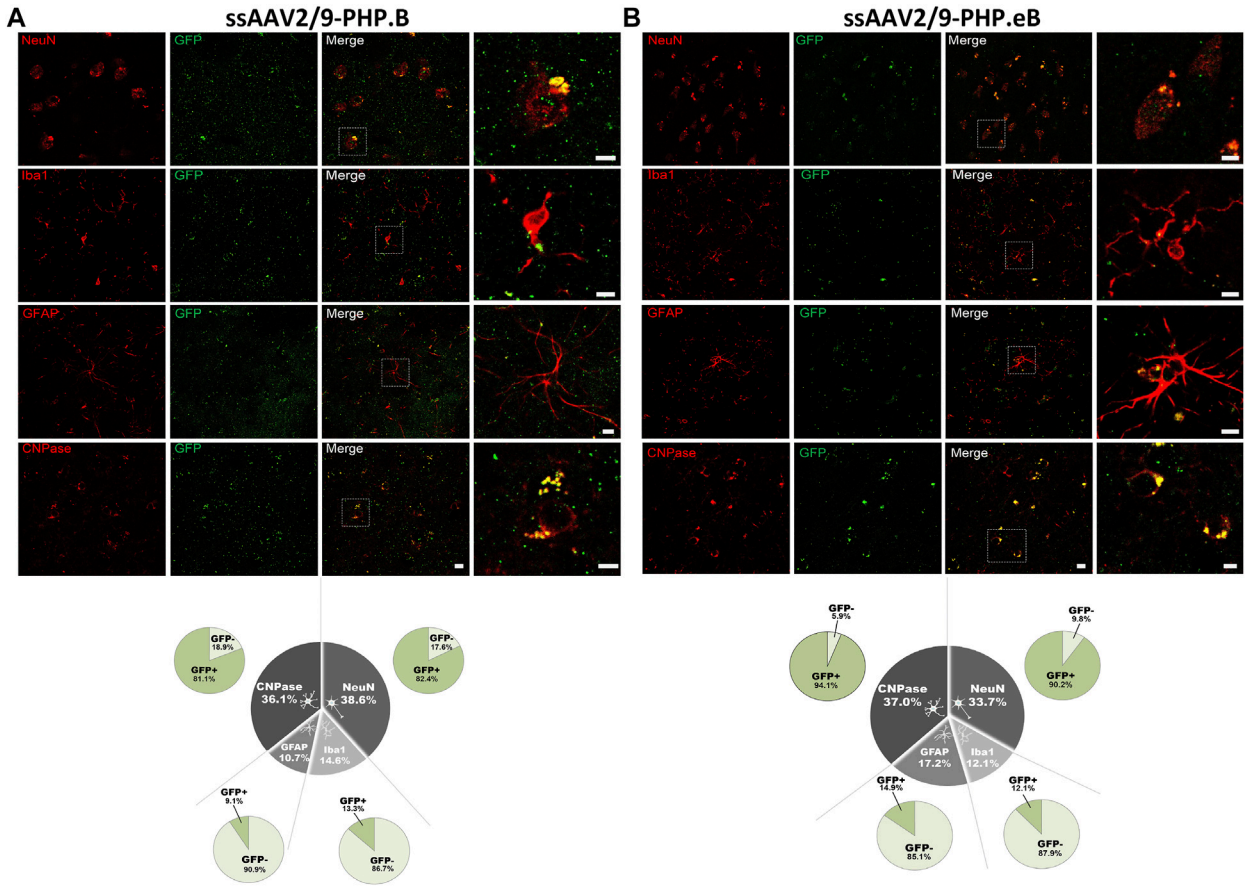


FIGURE 4 | Neuronal cell-type specificity resulting from AAV-PHP. B and AAV-PHP. eB injections in the putamen of non-human primates. **(A–B)** Representative images (top) and quantifications (down) of striatal sections from AAV-PHP. B-injected monkey **(A)** and AAV-PHP. eB-injected monkey **(B)** immunofluorescently labeled with anti-GFP antibody (green) and either a neuronal (NeuN), microglia (Iba1), astrocytic (GFAP + S-100) or oligodendroglial (CNPase) marker (red). Merging of the signals produced colocalization, thus confirming cellular transduction. Scale bar: 20 µm; 10 µm (high magnification). Quantitative analysis of percentage of cell types counted for each viral vector in the putamen of injected monkeys (grey) and percentage of cells transduced (dark green) or not (light green) per cell type.

labeling between EGFP and glial fibrillary acidic protein (GFAP; astrocyte-specific cellular marker) or with the microglia-specific cellular marker, ionized calcium-binding adapter molecule 1(Iba-1) was also observed (**Figures 4A,B**). A quantitative unbiased counting evaluated the total number of EGFP-transduced cells and EGFP-negative cells (**Table 2**). For both variants, we confirmed that 80–90% EGFP-positive cells were approximately co-labeled with NeuN, 12–13% with Iba1, 10–15% with GFAP, and 80–90% with CNPase in the putamen (**Figures 4A,B**, bottom).

Both Vectors Preferentially Targets Neurons in the Hippocampus

To assess whether the neuronal and oligodendroglial tropism observed in the putamen was also identical in other brain regions with a different distribution of cell types, we investigated the cellular transgene expression of EGFP in the hippocampus of both the AAV-PHP. B (**Figure 5A**) and AAV-PHP. eB (**Figure 5B**) condition (**Table 2**). While the neuronal tropism remained sustained for both variants in the hippocampus (with 89–90% of EGFP-positive cells that were co-labeled with NeuN), we observed a higher astrocytic transduction for both variants (with 57–61% of EGFP-positive cells that were co-labeled with GFAP/S100) and a lower oligodendroglial transduction, especially for the AAV-PHP. B variant (with 38–62% of EGFP-positive cells that were co-labeled with CNPase) in the hippocampus compared to the putamen (**Figures 5A,B**). These data demonstrate that intrathecal delivery of both AAV-PHP. B and AAV-PHP. eB leads predominantly to neuronal transduction and is region-specific for oligodendrocyte and glial tropism.

Both Vectors Achieved Weak GFP Transduction in the Spinal Cord and Liver

While intrathecal delivery leads to convincing forebrain transduction, EGFP-immunopositive cells and fibers were weakly labeled in the cervical, thoracic, and lumbar spinal cord segments in both AAV-PHP. B and AAV-PHP. eB conditions (**Figure 6A**). As expected with an intrathecal delivery, weak EGFP-positive expression was detected in the liver regardless of the virus subtype (**Figure 6B**),

TABLE 2 | Quantification of putaminal and hippocampal cell type distribution.

	Putamen						Hippocampus					
	AAV.PHP.B			AAV.PHP.eB			AAV.PHP.B			AAV.PHP.eB		
	GFP –	GFP+	Total	GFP –	GFP+	Total	GFP –	GFP+	Total	GFP –	GFP+	Total
NeuN	21	98	119	9	83	92	12	104	116	14	110	124
Iba1	39	6	45	29	4	33	26	10	36	28	15	43
GFAP	30	3	33	40	7	47	33	51	84	36	47	83
CNPase	21	90	111	6	95	101	20	12	32	27	44	71

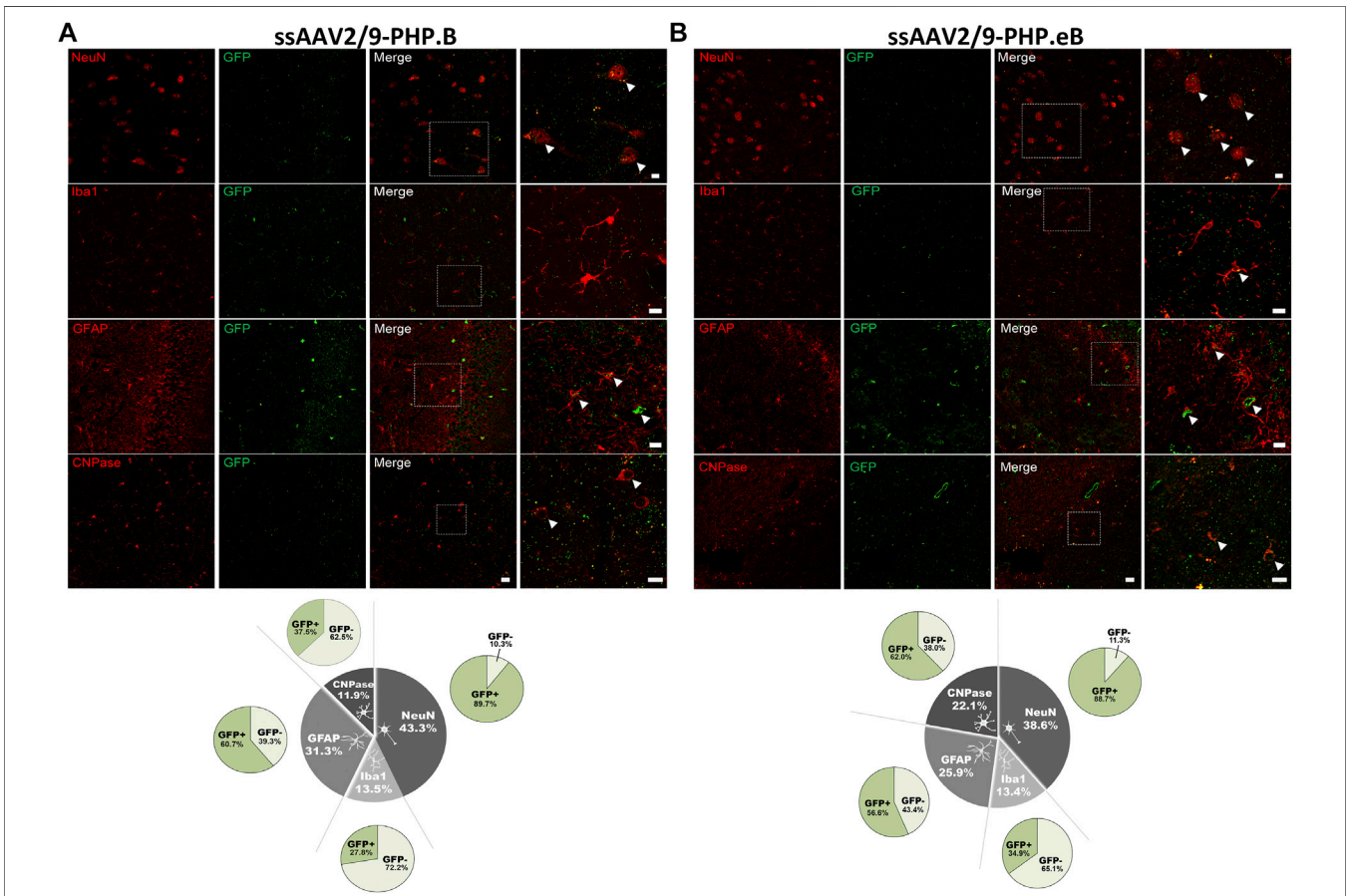


FIGURE 5 | Assessment of the cell-type specificity resulting from AAV-PHP. B and AAV-PHP. eB injections in the hippocampus of non-human primates. **(A–B)** Representative images (up) and quantifications (down) of striatal sections from AAV-PHP. B-injected monkey **(A)** and AAV-PHP. eB-injected monkey **(B)** immunofluorescently labeled with anti-GFP antibody (green) and either a neuronal (NeuN), microglia (Iba1), astrocytic (GFAP + S-100) or oligodendroglial (CNPase) marker (red). Merging of the signals produced colocalization, thus confirming cellular transduction. Scale bar: 20 µm; 10 µm (high magnification). White arrows represent the AAV-GFP transduced cells. Quantitative analysis of percentage of cell types counted for each viral vector in the hippocampus of injected monkeys (grey) and percentage of cells transduced (dark green) or not (light green) per cell type.

suggesting that transduction remained primarily limited to CNS.

DISCUSSION

To date, no studies have tested AAV-PHP. eB alone and compared AAV-PHP. B *vs.* AAV-PHP. eB variants in NHPs. This pilot study evaluated an unmet face-to-face evaluation of a single administration of equal doses of AAV-PHP. B and AAV-PHP. eB (1.5×10^{11} vg/ kg) to determine the potential use of those AAV9-derived variants in NHPs to transduce neural cells throughout the CNS, as successfully observed in rodents (Bedbrook et al., 2018). We decided to select one scalable and relatively noninvasive route of administration. Several reports have shown that intrathecal delivery of AAV vectors can enhance CNS penetration and optimize the ratio of CNS versus

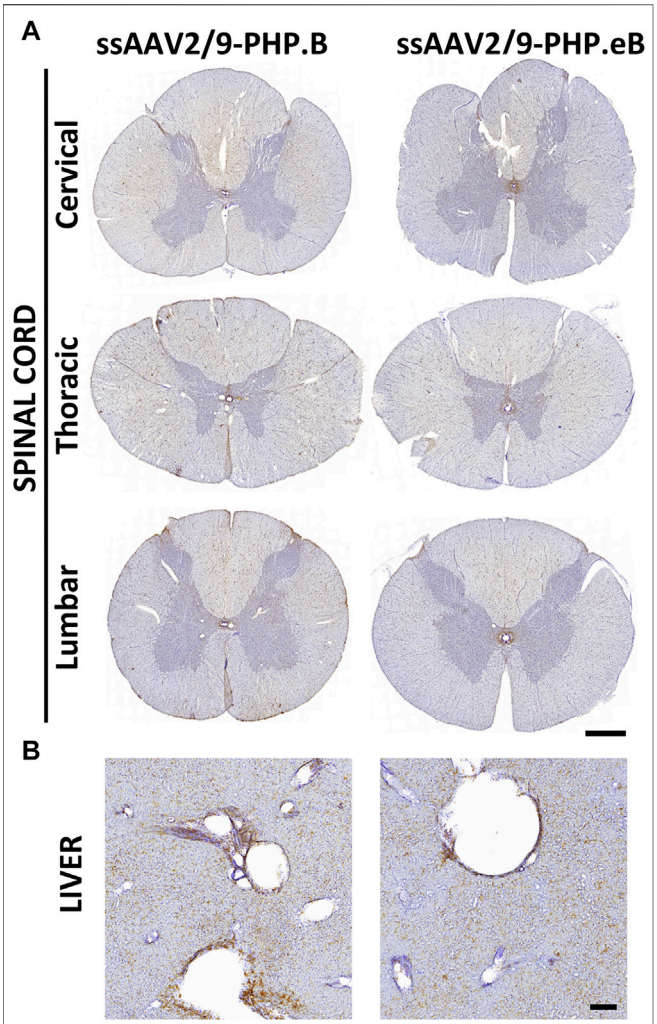


FIGURE 6 | Broad transduction of the spinal cord and liver resulting from AAV-PHP. B and AAV-PHP. eB injections in non-human primates. **(A)** Representative image of spinal cord sections at three levels (cervical, thoracic, lumbar) immunostained with EGFP in both injected monkeys. Scale bar: 1 mm. **(B)** Representative image of liver sections immunostained with a GFP antibody in both injected monkeys. Scale bar: 200 µm.

peripheral transduction (Gray et al., 2013; Castle et al., 2018; Hinderer et al., 2018; Liguore et al., 2019; Mathiesen et al., 2020). This minimally invasive intrathecal gene delivery system has the advantage of avoiding the occurrence of inflammation in the region surrounding the injection site during intracerebral injection. Moreover, intrathecal delivery of AAV2/9-gene therapies has been employed in clinical trials to treat giant axonal neuropathy (Bailey et al., 2018) and spinal muscular atrophy (Federici et al., 2012; Passini et al., 2014). Using a CAG promoter, which is ubiquitous and strong, to drive EGFP expression in both vectors, we observed widespread CNS transduction throughout the brain of both AAV-PHP. B- and AAV-PHP. eB-infused animals. Our study highlighted the superiority of AAV-PHP. eB CNS tropism and a more intense expression of EGFP than AAV-PHP. B in rhesus macaques. In addition, similar cell population-specific targeting was observed for both variants, mainly represented in neurons in the putamen and the hippocampus, while the transduction in non-neuronal cells seems to be more region-specific. Recently, (Matsuzaki et al., 2018) reported the lack of CNS tropism of AAV-PHP. B in the marmoset monkeys after i.v. administration at a dose of 5.0×10^{13} vg/ kg, questioning either the choice of the route of administration or differences between NHP species regarding the AAV transduction efficiency. In addition, (Hordeaux et al., 2018) reported that AAV-PHP. B did not enhance transduction in the rhesus macaque brain following i.v. injection. On the contrary, we reported here the transduction of neurons in the brain of the rhesus macaques, even at a 130-fold lower dose than the dose used by the authors (1.5×10^{11} vg/ kg compared with 2.0×10^{13} vg/ kg). Lately, (Liguore et al., 2019) evaluated transduction efficiency of AAV-PHP. B (but not AAV-PHP.eB) in the rhesus macaque following four distinct injection strategies. Following intrathecal administration at a dose of 1.0×10^{12} vg/kg, they observed broad cortical and spinal cord transduction, supporting our findings. Recently, (Galvan et al., 2021) demonstrated that a single intracerebroventricular injection of AAV9-PHP.B in two adult rhesus macaques (1.87×10^{12} vg/ kg and 3.95×10^{12} vg/ kg)., using a gene promoter that confers high neuron-specific expression of the transgene, the human synapsin 1 (SYN1), to drive the expression of emerald green fluorescent protein (EmGFP) in neurons, was efficient to induce widespread transgene expression in various populations of cortical and subcortical neurons in the primate brain.

While this first data set is encouraging, pending questions await future investigation before translating our findings to eventual use in gene therapy applications. We believe that it is crucial to accomplish several additional experiments on NHPs to lay a critical ground for a more systematic investigation in the CNS, peripheral (PNS), and enteric (ENS) nervous systems. Careful studies are needed to determine the precise pathological and molecular mechanisms involved and the potential implication for clinical trials using comparable doses of systemic vectors. Further investigations with those AAV9 capsid variants, particularly with the less characterized AAV-PHP. eB, should be conducted with additional animals to reach statistical power. Towards this goal, we propose different aspects of refinement that can be studied in a full-scale study in the near future. First, age should be considered as a variable (juvenile *vs*. mature), and inherent differences might exist in how AAV-PHP. B and AAV-PHP. eB transduce rhesus macaque brain. Second, single versus multiple injections may allow improving biodistribution throughout the brain. Third, the dose may be a crucial parameter, as in one NHP study, using AAV-PHP. B at a dose of 7.5×10^{13} vg/ kg led to unexpected AAV-mediated toxicity after a single i.v. injection (Hordeaux et al., 2018). Fourth, the specificity of expression being driven by structure or cellular-specific promoters within the vector genome should also be considered a way to control what cell types and under what conditions the transgene is expressed (Smith et al., 2021).

Altogether, this proof-of-concept experiment demonstrates that AAV-PHP. B and AAV-PHP. eB are robust viral vectors for gene transfer, notably to the brain, providing a promising research tool for delivering genes to NHPs. The present data have broad implications in brain

diseases and constitute a dramatic step toward using engineered AAV9 capsid variants vectors to model human disease onset and deliver gene therapies to the CNS in humans. Interestingly, in the field of synucleinopathies, where neurons and oligodendrocytes are the primary cells involved in Parkinson's disease and multiple system atrophy, respectively, the use of those viral vectors may be an attractive approach to target multiple affected brain cells. Regarding the field of tauopathy, the neuronal and oligodendroglial tropism of these vectors would be of interest to model four-repeat (4R-) tauopathies, for instance (progressive supranuclear palsy (PSP) and corticobasal degeneration (CBD), where neuronal inclusions and coiled bodies are hallmarks of the disease (Rosler et al., 2019).

DATA AVAILABILITY STATEMENT

The raw data supporting the conclusions of this article will be made available by the authors, without undue reservation.

ETHICS STATEMENT

The animal study was reviewed and approved by French Ethical Committee for Animal Research CE50.

AUTHOR CONTRIBUTIONS

M-LA, SD, NB, ND, and VP performed the experiments, analyzed and interpreted the data. EB proofread the manuscript. BD conceived and designed the experiments; performed the experiments; analyzed and interpreted the data. M-LA and BD wrote the paper. BD is corresponding author. BD and EB secured the funding. All authors read and approved the manuscript.

FUNDING

M-LA was the recipient of a MESR fellowship and the France Parkinson Foundation. The University of Bordeaux, and the Centre National de la Recherche Scientifique provided infrastructural support.

ACKNOWLEDGMENTS

We thank Dr. Gregory Porras, Marie-Laure Thiolat, Tho Hai Nguyen, and Hugues Orignac for their invaluable help in conducting the reported experiments. Accommodations and experiments were performed in the Service des Animaleries of the University of Bordeaux, supported by the Région Aquitaine.

REFERENCES

Allen, W. E., Kauvar, I. V., Chen, M. Z., Richman, E. B., Yang, S. J., Chan, K., et al. (2017). Global Representations of Goal-Directed Behavior in Distinct Cell Types of Mouse Neocortex. *Neuron* 94, 891–907. doi:10.1016/j.neuron.2017.04.017

Aurnhammer, C., Haase, M., Muether, N., Hausl, M., Rauschhuber, C., Huber, I., et al. (2012). Universal Real-Time PCR for the Detection and Quantification of Adeno-Associated Virus Serotype 2-derived Inverted Terminal Repeat Sequences. *Hum. Gene Ther. Methods* 23, 18–28. doi:10.1089/hgtb.2011.034

Bailey, R. M., Armao, D., Nagabhushan Kalburgi, S., and Gray, S. J. (2018). Development of Intrathecal AAV9 Gene Therapy for Giant Axonal Neuropathy. *Mol. Ther. - Methods Clin. Dev.* 9, 160–171. doi:10.1016/j.omtm.2018.02.005

Bedbrook, C. N., Deverman, B. E., and Gradinaru, V. (2018). Viral Strategies for Targeting the Central and Peripheral Nervous Systems. *Annu. Rev. Neurosci.* 41, 323–348. doi:10.1146/annurev-neuro-080317-062048

Bey, K., Deniaud, J., Dubreil, L., Joussemet, B., Cristini, J., Ciron, C., et al. (2020). Intra-CSF AAV9 and AAVrh10 Administration in Nonhuman Primates: Promising Routes and Vectors for Which Neurological Diseases? *Mol. Ther. - Methods Clin. Dev.* 17, 771–784. doi:10.1016/j.omtm.2020.04.001

Bourdenx, M., Dutheil, N., Bezard, E., and Dehay, B. (2014). Systemic Gene Delivery to the central Nervous System Using Adeno-Associated Virus. *Front. Mol. Neurosci.* 7, 50. doi:10.3389/fnmol.2014.00050

Castle, M. J., Cheng, Y., Asokan, A., and Tuszynski, M. H. (2018). Physical Positioning Markedly Enhances Brain Transduction after Intrathecal AAV9 Infusion. *Sci. Adv.* 4, eaau9859. doi:10.1126/sciadv.aau9859

Cearley, C. N., and Wolfe, J. H. (2006). Transduction Characteristics of Adeno-Associated Virus Vectors Expressing Cap Serotypes 7, 8, 9, and Rh10 in the Mouse Brain. *Mol. Ther.* 13, 528–537. doi:10.1016/j.ymthe.2005.11.015

Chan, K. Y., Jang, M. J., Yoo, B. B., Greenbaum, A., Ravi, N., Wu, W.-L., et al. (2017). Engineered AAVs for Efficient Noninvasive Gene Delivery to the central and Peripheral Nervous Systems. *Nat. Neurosci.* 20, 1172–1179. doi:10.1038/nn.4593

Chansel-Debordeaux, L., Bourdenx, M., Dovero, S., Grouthier, V., Dutheil, N., Espana, A., et al. (2017). In Utero Delivery of rAAV2/9 Induces Neuronal Expression of the Transgene in the Brain: towards New Models of Parkinson's Disease. *Gene Ther.* 24, 801–809. doi:10.1038/gt.2017.84

Chansel-Debordeaux, L., Bourdenx, M., Dutheil, N., Dovero, S., Canron, M.-H., Jimenez, C., et al. (2018). Systemic Gene Delivery by Single-Dose Intracardiac Administration of scAAV2/9 and scAAV2/rh10 Variants in Newborn Rats. *Hum. Gene Ther. Methods* 29, 189–199. doi:10.1089/hgtb.2017.192.r3

Chatterjee, D., Marmion, D. J., Mcbride, J. L., Manfredsson, F. P., Butler, D., Messer, A., et al. (2021). Enhanced CNS Transduction from AAV.PHP.eB Infusion into the Cisterna Magna of Older Adult Rats Compared to AAV9. *Gene Ther.* doi:10.1038/s41434-021-00244-y

Dayton, R. D., Grames, M. S., and Klein, R. L. (2018). More Expansive Gene Transfer to the Rat CNS: AAV PHP.EB Vector Dose-Response and Comparison to AAV PHP.B. *Gene Ther.* 25, 392–400. doi:10.1038/s41434-018-0028-5

Dehay, B., Dalkara, D., Dovero, S., Li, Q., and Bezard, E. (2012). Systemic scAAV9 Variant Mediates Brain Transduction in Newborn Rhesus Macaques. *Sci. Rep.* 2, 253. doi:10.1038/srep00253

Deverman, B. E., Pravdo, P. L., Simpson, B. P., Kumar, S. R., Chan, K. Y., Banerjee, A., et al. (2016). Cre-dependent Selection Yields AAV Variants for Widespread Gene Transfer to the Adult Brain. *Nat. Biotechnol.* 34, 204–209. doi:10.1038/nbt.3440

Deverman, B. E., Ravina, B. M., Bankiewicz, K. S., Paul, S. M., and Sah, D. W. Y. (2018). Gene Therapy for Neurological Disorders: Progress and Prospects. *Nat. Rev. Drug Discov.* 17, 641–659. doi:10.1038/nrd.2018.110

Duque, S., Joussemet, B., Riviere, C., Marais, T., Dubreil, L., Douar, A.-M., et al. (2009). Intravenous Administration of Self-Complementary AAV9 Enables Transgene Delivery to Adult Motor Neurons. *Mol. Ther.* 17, 1187–1196. doi:10.1038/mt.2009.71

Fajardo-Serrano, A., Rico, A. J., Roda, E., Honrubia, A., Arrieta, S., Ariznabarreta, G., et al. (2021). Adeno-Associated Viral Vectors as Versatile Tools for Parkinson's Research, Both for Disease Modeling Purposes and for Therapeutic Uses. *Int. J. Mol. Sci.* 22, 6389. doi:10.3390/ijms22126389

Federici, T., Taub, J. S., Baum, G. R., Gray, S. J., Grieger, J. C., Matthews, K. A., et al. (2012). Robust Spinal Motor Neuron Transduction Following Intrathecal Delivery of AAV9 in Pigs. *Gene Ther.* 19, 852–859. doi:10.1038/gt.2011.130

Foust, K. D., Nurre, E., Montgomery, C. L., Hernandez, A., Chan, C. M., and Kaspar, B. K. (2009). Intravascular AAV9 Preferentially Targets Neonatal Neurons and Adult Astrocytes. *Nat. Biotechnol.* 27, 59–65. doi:10.1038/nbt.1515

Galvan, A., Petkau, T. L., Hill, A. M., Korecki, A. J., Lu, G., Choi, D., et al. (2021). Intracerebroventricular Administration of AAV9-PHP.B SYN1-EmGFP Induces Widespread Transgene Expression in the Mouse and Monkey Central Nervous System. *Hum. Gene Ther.* 32, 599–615. doi:10.1089/hum.2020.301

Gao, Y., Geng, L., Chen, V. P., and Brimijoin, S. (2017). Therapeutic Delivery of Butyrylcholinesterase by Brain-Wide Viral Gene Transfer to Mice. *Molecules* 22, 1145. doi:10.3390/molecules22071145

Gray, S. J., Nagabhushan Kalburgi, S., Mccown, T. J., and Jude Samulski, R. (2013). Global CNS Gene Delivery and Evasion of Anti-AAV-neutralizing Antibodies by Intrathecal AAV Administration in Non-human Primates. *Gene Ther.* 20, 450–459. doi:10.1038/gt.2012.101

Hinderer, C., Bell, P., Vite, C. H., Louboutin, J.-P., Grant, R., Bote, E., et al. (2014). Widespread Gene Transfer in the central Nervous System of Cynomolgus Macaques Following Delivery of AAV9 into the Cisterna magna. *Mol. Ther. - Methods Clin. Dev.* 1, 14051. doi:10.1038/mtm.2014.51

Hinderer, C., Bell, P., Katz, N., Vite, C. H., Louboutin, J.-P., Bote, E., et al. (2018). Evaluation of Intrathecal Routes of Administration for Adeno-Associated Viral Vectors in Large Animals. *Hum. Gene Ther.* 29, 15–24. doi:10.1089/hum.2017.026

Hordeaux, J., Wang, Q., Katz, N., Buza, E. L., Bell, P., and Wilson, J. M. (2018). The Neurotropic Properties of AAV-PHP.B Are Limited to C57BL/6J Mice. *Mol. Ther.* 26, 664–668. doi:10.1016/j.ymthe.2018.01.018

Hudry, E., and Vandenberghe, L. H. (2019). Therapeutic AAV Gene Transfer to the Nervous System: A Clinical Reality. *Neuron* 101, 839–862. doi:10.1016/j.neuron.2019.02.017

Jackson, K. L., Dayton, R. D., Deverman, B. E., and Klein, R. L. (2016). Better Targeting, Better Efficiency for Wide-Scale Neuronal Transduction with the Synapsin Promoter and AAV-PHP.B. *Front. Mol. Neurosci.* 9, 116. doi:10.3389/fnmol.2016.00116

Liguore, W. A., Domire, J. S., Button, D., Wang, Y., Dufour, B. D., Srinivasan, S., et al. (2019). AAV-PHP.B Administration Results in a Differential Pattern of CNS Biodistribution in Non-human Primates Compared with Mice. *Mol. Ther.* 27, 2018–2037. doi:10.1016/j.ymthe.2019.07.017

Mathiesen, S. N., Lock, J. L., Schoderboeck, L., Abraham, W. C., and Hughes, S. M. (2020). CNS Transduction Benefits of AAV-PHP.eB over AAV9 Are Dependent on Administration Route and Mouse Strain. *Mol. Ther. - Methods Clin. Dev.* 19, 447–458. doi:10.1016/j.omtm.2020.10.011

Matsuzaki, Y., Konno, A., Mochizuki, R., Shinohara, Y., Nitta, K., Okada, Y., et al. (2018). Intravenous Administration of the Adeno-Associated virus-PHP.B Capsid Fails to Upregulate Transduction Efficiency in the Marmoset Brain. *Neurosci. Lett.* 665, 182–188. doi:10.1016/j.neulet.2017.11.049

Morabito, G., Giannelli, S. G., Ordazzo, G., Bido, S., Castoldi, V., Indrigo, M., et al. (2017). AAV-PHP.B-Mediated Global-Scale Expression in the Mouse Nervous System Enables GBA1 Gene Therapy for Wide Protection from Synucleinopathy. *Mol. Ther.* 25, 2727–2742. doi:10.1016/j.ymthe.2017.08.004

Nectow, A. R., and Nestler, E. J. (2020). Viral Tools for Neuroscience. *Nat. Rev. Neurosci.* 21, 669–681. doi:10.1038/s41583-020-00382-z

Passini, M. A., Bu, J., Richards, A. M., Treleaven, C. M., Sullivan, J. A., O'riordan, C. R., et al. (2014). Translational Fidelity of Intrathecal Delivery of Self-Complementary AAV9-Survival Motor Neuron 1 for Spinal Muscular Atrophy. *Hum. Gene Ther.* 25, 619–630. doi:10.1089/hum.2014.011

Rincon, M. Y., De Vin, F., Duqué, S. I., Fripont, S., Castaldo, S. A., Bouhuijzen-Wenger, J., et al. (2018). Widespread Transduction of Astrocytes and Neurons in the Mouse central Nervous System after Systemic Delivery of a Self-Complementary AAV-PHP.B Vector. *Gene Ther.* 25, 83–92. doi:10.1038/s41434-018-0005-z

Rösler, T. W., Tayaranian Marvian, A., Brendel, M., Nykänen, N.-P., Höllerhage, M., Schwarz, S. C., et al. (2019). Four-repeat Tauopathies. *Prog. Neurobiol.* 180, 101644. doi:10.1016/j.pneurobio.2019.101644

Samaranch, L., Salegio, E. A., San Sebastian, W., Kells, A. P., Bringas, J. R., Forsayeth, J., et al. (2013). Strong Cortical and Spinal Cord Transduction after AAV7 and AAV9 Delivery into the Cerebrospinal Fluid of Nonhuman Primates. *Hum. Gene Ther.* 24, 526–532. doi:10.1089/hum.2013.005

Smith, E. J., Farshim, P. P., Flomen, R., Jones, S. T., Mcateer, S. J., Deverman, B. E., et al. (2021). Use of High-Content Imaging to Quantify Transduction of AAV-PHP Viruses in the Brain Following Systemic Delivery. *Brain Commun.* 3, fcab105. doi:10.1093/braincomms/fcab105

Xiao, X., Li, J., and Samulski, R. J. (1998). Production of High-Titer Recombinant Adeno-Associated Virus Vectors in the Absence of Helper Adenovirus. *J. Virol.* 72, 2224–2232. doi:10.1128/jvi.72.3.2224-2232.1998

Yang, B., Li, S., Wang, H., Guo, Y., Gessler, D. J., Cao, C., et al. (2014). Global CNS Transduction of Adult Mice by Intravenously Delivered rAAVrh.8 and rAAVrh.10 and Nonhuman Primates by rAAVrh.10. *Mol. Ther.* 22, 1299–1309. doi:10.1038/mt.2014.68

Zhang, H., Yang, B., Mu, X., Ahmed, S. S., Su, Q., He, R., et al. (2011). Several rAAV Vectors Efficiently Cross the Blood-Brain Barrier and Transduce Neurons and Astrocytes in the Neonatal Mouse central Nervous System. *Mol. Ther.* 19, 1440–1448. doi:10.1038/mt.2011.98

Zolotukhin, S., Potter, M., Zolotukhin, I., Sakai, Y., Loiler, S., Fraites, T. J., Jr., et al. (2002). Production and Purification of Serotype 1, 2, and 5 Recombinant Adeno-Associated Viral Vectors. *Methods* 28, 158–167. doi:10.1016/s1046-2023(02)00220-7

Conflict of Interest: EB owns an equity stake in Motac holding Ltd and receives consultancy payments from Motac Neuroscience Ltd.

The remaining authors declare that the research was conducted in the absence of any commercial or financial relationships that could be construed as a potential conflict of interest.

Publisher's Note: All claims expressed in this article are solely those of the authors and do not necessarily represent those of their affiliated organizations, or those of the publisher, the editors and the reviewers. Any product that may be evaluated in this article, or claim that may be made by its manufacturer, is not guaranteed or endorsed by the publisher.

Copyright © 2021 Arotcarena, Dovero, Biendon, Dutheil, Planche, Bezard and Dehay. This is an open-access article distributed under the terms of the Creative Commons Attribution License (CC BY). The use, distribution or reproduction in other forums is permitted, provided the original author(s) and the copyright owner(s) are credited and that the original publication in this journal is cited, in accordance with accepted academic practice. No use, distribution or reproduction is permitted which does not comply with these terms.